PCCP

Accepted Manuscript

ROYAL SOCIETY OF CHEMISTRY

www.rsc.org/pccp

Looking inside the pores of a MCM-41 based Mo heterogeneous styrene oxidation catalyst: an inelastic neutron scattering study

Cristina I. Fernandes,[a] Svemir Rudić,[b] Pedro D. Vaz,[*a,b] Carla D. Nunes[*a]

[a] CQB, Departamento de Química e Bioquímica, Faculdade de Ciências da Universidade de Lisboa, 1749-016 Lisboa, Portugal

[b] ISIS Neutron & Muon Source, Rutherford Appleton Laboratory, Chilton, Didcot, Oxfordshire OX11 0QX, United Kingdom

Corresponding authors

Dr. Carla D. Nunes

CQB, Departamento de Química e Bioquímica, Faculdade de Ciências da Universidade de Lisboa, 1749-016 Lisboa, Portugal

Tel: +351-217500876

Fax: (+351) 217 500088

E-mail: cmnunes@ciencias.ulisboa.pt

or

Dr. Pedro D. Vaz

Centro de Química e Bioquímica, Departamento de Química e Bioquímica, Faculdade de Ciências da Universidade de Lisboa, 1749-016 Lisboa, Portugal

Tel: +351-217500877

Fax: (+351) 217500088

E-mail: pmvaz@ciencias.ulisboa.pt

Abstract

Styrene oxidation mediated by a Mo-based mesoporous catalyst can yield selectively styrene oxide or benzaldehyde. Kinetic data evidenced that styrene oxide is the initially single-product formed by the catalytic Mo-mediated process. However, after some hours of reaction benzaldehyde yield rises while that of the epoxide decreases concomitantly. The mechanistic proposal pointed out to a surface assisted acid-base mechanism by which styrene oxide is interconverted into benzaldehyde through over-oxidation and cleavage of the C–C bond and releasing formaldehyde as well. In an attempt to gain some insight on whether this

mechanistic proposal is realistic we have conducted a combined DRIFT and inelastic neutron scattering (INS) study to assess the adsorbed species at the catalyst's surface and confirm the mechanistic proposal. INS and DRIFT provided complementary insight into surface-adsorbed species by probing donor (INS) and acceptor (DRIFT) species. INS also allowed for an estimation of product selectivity by means of a Job method stressing the power of the technique.

1. Introduction

Heterogeneous catalysts receive considerable attention due to their superior properties that make their use more convenient.[1-5] Such class of catalysts is advantageous over the homogeneous counterparts since they are easy to recover from the reaction slurry, making it the preferred approach in most industrial applications.[1,2] As a drawback, selectivity is usually lower than that of many homogeneous systems.[1] However, continuous efforts led to the development of newer generations of heterogeneous catalysts that can match and exceed properties of many homogeneous catalysts. Despite this, the design of more active and selective heterogeneous catalysts still remains a priority and a challenge.[6] Among different types of heterogeneous catalysts, MCM-41 type mesoporous materials meet many of the relevant criteria to fullfil this application.[3,5] Such materials can be used on their own, as active catalysts, or as supports for other species that will be the active part. In this case their role as support will be passive.

Achieving high product selectivity in a given process is the major challenge one faces in catalysis. Oxidation of olefins is a very active field of research both in academia and industry.[3-5] The oxidation of styrene is actively studied since its oxidation products, styrene oxide and benzaldehyde are relevant intermediaries in the production of fine chemicals and fragrances.[7-9] Another important reaction is the synthesis of benzaldehyde from benzyl alcohol; this transformation is challenging since usually it can originate not only the aldehyde, but also toluene or even benzoic acid (resulting from over-oxidation of the aldehyde).[10]

Over the recent years we have designed Mo-based heterogeneous catalysts that under mild conditions (temperatures in the range 328–373 K with *tert*-butylhydroperoxide as oxidant) yield selectively one or both products.[6] In fact the effect of inter-conversion of the epoxide into the aldehyde by means of an oxidative cleavage mechanism where the epoxide is further oxidized and consequently originating benzaldehyde and formaldehyde as a result of the cleavage of the C–C bond, was outlined in previous works.[11,12] Other catalytic systems do not offer such versatility of tuning product selectivity (alternating between the epoxide or aldehyde) as the Mo-based ones that we have reported so far.[13]

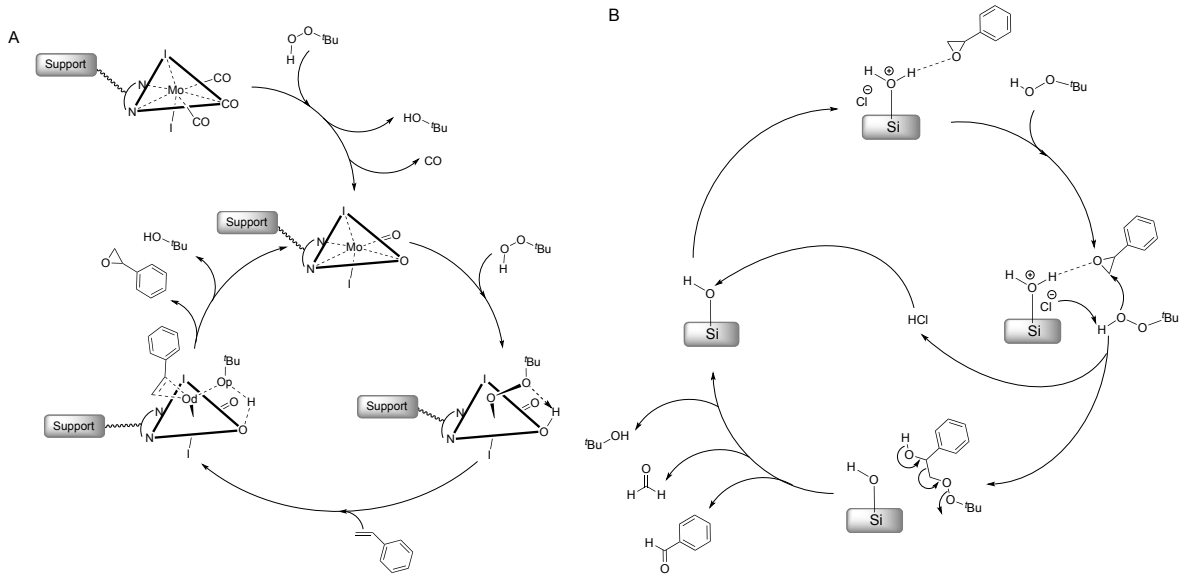

Scheme 1. Mechanism proposal for the catalytic styrene oxidation cycle yielding styrene oxide and benzaldehyde. A - Starting from an MCM-41 supported Mo^{II} pre-catalyst (in some steps the metal is omitted for clarity); in this part the Mo^{II} pre-catalyst is firstly oxidized to the Mo^{VI} active species. B – Mechanism proposal for the catalytic benzaldehyde formation from styrene oxide catalyzed by acid sites in the MCM-41 support.

In this work we have synthesized a Mo-based heterogenous catalysts supported on MCM-41 silica. The low Mo-loading gives this catalyst the behaviour of a single-site catalyst. This catalyst, in a similar fashion to others described earlier,[14,15] was found to yield, over a period of 24 h, styrene oxide (Scheme 1A) that after sometime starts to interconvert into benzaldehyde. The possible mechanism for this was described as a support assisted reaction where the MCM-41 surface is acting as an acid catalyst.[11,12] According to Scheme 1B, a styrene oxide molecule approaches an acid site and then a *tert*-butylhydroperoxide (tbhp) molecule reacts with the activated epoxide, with the concomitant release of an HCl molecule. The reaction yields benzaldehyde, formaldehyde and *tert*-butanol. In the final step the HCl molecule can regenerate the acid site closing the cycle for a new transformation. As part of ongoing research to assess whether such proposal is realistic we used in this study Diffuse Reflectance Infrared Fourier Transform (DRIFT) and Inelastic Neutron Scattering (INS) Spectroscopy as a complementary techniques. DRIFT spectroscopy is a widely available and well-understood technique for studies of heterogeneous catalysts. We have previously reported such technique in the study of related MCM-41 based materials to probe local structure.[16] In a similar way to Raman, INS relies on scattered neutrons by the atomic nuclei. The scattering intensity depends on the incoherent inelastic scattering cross section and the

amplitude of vibration. While both of these quantities are large for protium, they are small for all remaining nuclei present in this work; as such the scattered intensity is dominated by hydrogen motion. In this work we describe the findings of *in situ* spectroscopic studies of the MCM-41 immobilized Mo catalyst using INS and DRIFT. To the best of our knowledge, this is the first study dealing with the characterization of a selective Mo-based heterogeneous styrene oxidation catalyst by INS and DRIFT.

Experimental

Catalyst Preparation

All reagents were obtained from Aldrich and used as received. Commercial grade solvents were dried and deoxygenated by standard procedures distilled under nitrogen, and kept over 4 Å molecular sieves (3 Å for acetonitrile). The complex $[MoI_2(CO)_3(CH_3CN)_2]$ was prepared according to a literature method.[17] The $(ClCO)_2$bpy ligand (4,4′-dicarbonyl-2,2′-bipyridine chloride) was obtained from the corresponding carboxylic acid (4,4′-dicarboxylic-2,2′-bipyridine), which had previously been obtained by oxidation of the methyl derivative (4,4′-dimethyl-2,2′-bipyridine).[18]

MCM-41 was synthesized adopting a previously described methodology, using $[(C_{14}H_{33})N(CH_3)_3]Br$ as structure directing agent.[19] To remove the surfactant, the MCM-41 material (3 g) was added to a solution of MeOH (250 mL) and HCl 36% (6.0 g). After stirring for 6 h at 323 K the solid was filtered off and dried in vacuum during 2 h. This procedure was accomplished twice to ensure that all the surfactant was removed.

Prior to the grafting experiments, physisorbed water was removed from the materials by heating at 453 K in vacuum (10^{-2} Pa) for 2 h.

Material MCM-bpy resulted from the addition of a suspension of the $(ClCO)_2$bpy ligand (1.405 g; 5 mmol) in acetonitrile (CH_3CN) to a suspension of MCM (5.0 g) in acetonitrile (CH_3CN), and the mixture was heated at 358 K for 14 h. The resulting solid was filtered off and washed twice with dichloromethane (CH_2Cl_2), then dried in vacuum at 323 K for 2 h.

MCM-bpy-Mo material (the catalyst) was obtained by adding a solution of $[MoI_2(CH_3CN)_2(CO)_3]$ (1.50 g, 2.8 mmol) in dry dichloromethane (CH_2Cl_2) to a suspension of 5 g of MCM-bpy material in dry dichloromethane (CH_2Cl_2). The reaction mixture was stirred under a N_2 atmosphere at room temperature for 14 h. The resulting material was then filtered off, washed twice with dichloromethane (CH_2Cl_2), and dried under vacuum for 3 h.

Catalyst Characterization

FTIR spectra were obtained as Diffuse Reflectance Infrared Spectroscopy (DRIFT) measurements on a Nicolet 6700 in the 400−4000 cm^{-1} range using 4 cm^{-1} resolution. Powder XRD measurements were taken on a Philips Analytical PW 3050/60 X'Pert PRO (theta/2 theta) equipped with X'Celerator detector and with automatic data acquisition (X'Pert Data Collector (v2.0b) software), using a monochromatized Cu-Kα radiation as incident beam, using 40 kV and 30 mA.

The N_2 sorption measurements were obtained on a Quantachrome Autosorb iQ porosimeter. BET specific surface areas (S_{BET}, P/P_0 from 0.03 to 0.30) and specific total pore volume V_p were estimated from N_2 adsorption isotherms measured at 77 K. The pore size distributions (PSD) were calculated by the Barrett-Joyner-Halenda (BJH) method from the desorption branch of the isotherm, using the modified Kelvin equation with correction for the statistical film thickness on the pore walls.[20,21] The statistical film thickness was calculated using Harkins–Jura equation in the p/p_0 range from 0.1 to 0.95.

Microanalyses for CHN and Mo quantification were performed at CACTI, University of Vigo. CHN analyses were performed on a Fisons EA 1108; Mo quantification was performed on a Perkin Elmer Optima 4300DV using In as internal standard.

Catalytic tests

The catalytic oxidation of styrene was carried out at 353 K under air in a reaction vessel equipped with a magnetic stirrer and a condenser. In a typical experiment the vessel was loaded with styrene (100 mol%), internal standard (dibutyl ether, dbe), catalyst (1 mol%), oxidant (200 mol%) and 3 mL of acetonitrile as solvent. The final volume of the reaction is ca. 6 mL. Addition of the oxidant determines the initial time of the reaction. Conversion and product yields were monitored by sampling periodically. Samples were analysed using a Shimadzu QP2100-Plus GC/MS system and a capillary column (Teknokroma TRB-5MS) operating in the linear velocity mode.

Inelastic neutron scattering (INS) spectroscopy

Inelastic neutron scattering spectra were recorded on the TOSCA spectrometer at the ISIS Pulsed Neutron and Muon Source at the Rutherford Appleton Laboratory, Chilton, UK.[22] TOSCA is a high resolution, broad range, inverse geometry spectrometer well suited to the spectroscopy of hydrogenous materials. The energy transfer range is from -24 to 8000 cm^{-1}.

The resolution is $\Delta E/E \sim 1.5\%$. The oxidation reactions for the spectroscopic studies (DRIFT and INS) were carried out inside TiZr flow through cans. The catalyst samples were loaded inside the cans between quartz wool. The cans were sealed and heated to 353 K. Then the inlet line of the can was connected to the helium gas supply and left for period of 12 h at a temperature of 393 K to remove any absorbed species. Styrene and tbhp vapours were dosed onto the surface of the catalyst at 353 K for a period of 4 h. The dosing system consisted of a He line going through a heated styrene/tbhp mixture (333 K) reservoir. After that time the cans were flushed for 1 h with He to remove excess species in the vapor phase that would be weakly or not adsorbed at all.

The cans were then mounted on a regular TOSCA centre stick, loaded into TOSCA and cooled down to a temperature below 15 K. Each catalyst spectrum was recorded until good statistics was achieved.

The spectra of the reference materials – styrene, styrene oxide and benzaldehyde – were measured in standard 2 mm thick TOSCA flat cans at ca. 15 K.

Results and discussion

Synthesis and characterization of heterogeneous Mo catalyst

The synthetic procedure adopted to prepare the Mo-based mesoporous heterogeneous catalyst is outlined in Scheme 2.

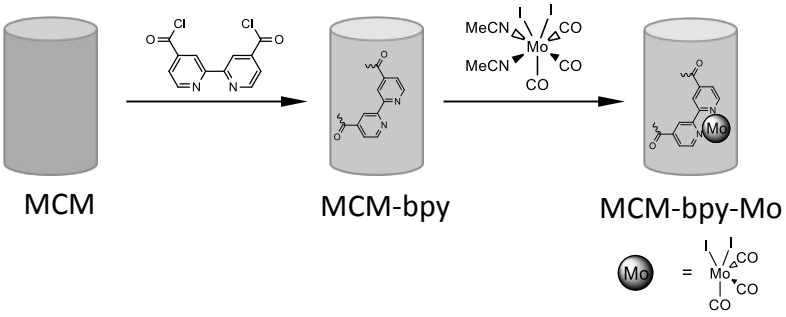

Scheme 2. Synthetic procedure for preparation of the Mo heterogeneous catalyst.

Regular MCM-41 (hereafter denoted MCM) type mesostructured silica material was prepared using myristyltrimethylammonium bromide (C_{14}TAB) as surfactant, according to a literature procedure [35].

Afterwards a bipyridine derivative (bpy) (Scheme 2) was used as ligand to coordinate Mo^{II} centres after being grafted to the inner silanol surface of the material. Grafting of bpy ligand

was straightforward by reacting $(ClCO)_2$bpy with a suspension of MCM in acetonitrile, yielding MCM-bpy. Subsequently, the Mo organometallic core was introduced by suspending the MCM-bpy material in dichloromethane and then adding the precursor complex, $[MoI_2(CO)_3(CH_3CN)_2]$, affording MCM-bpy-Mo. From elemental analysis the Mo content was found to be 4.36%, corresponding to 0.45 mmol·g^{-1} while CHN analyses for MCM-bpy-Mo revealed values of 7.34 % C, 1.37 % H and 0.98 % N. Based on the N content, these results also show that the loading of bpy derivative inside the pores is 0.6 mmol·g^{-1}. Textural properties were assessed by powder XRD and sorption/desorption N_2 isotherms were also carried out for textural parameters estimation. All resulting materials were of good quality according to the X-ray diffraction (XRD) powder patterns (Fig. 1).

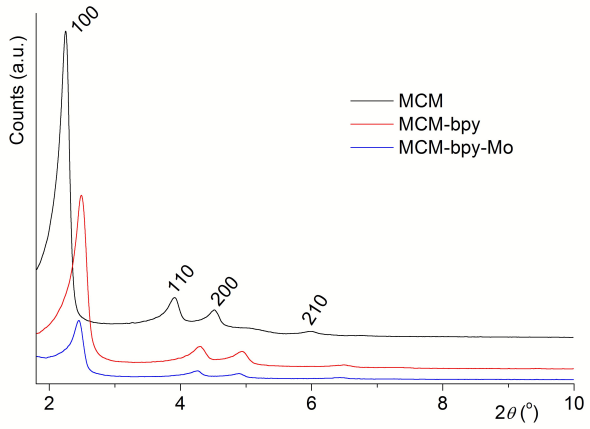

Figure 1. XRD powder patterns of MCM, MCM-bpy and MCM-bpy-Mo materials.

The XRD powder patterns (Fig. 1) of the MCM pristine material exhibited four reflections indexed to a hexagonal cell as (100), (110), (200) and (210) in the $2 < 2\theta < 10^{\circ}$ range. For that material the d_{100} value for reflection (100) is estimated to be 39.0 Å, corresponding to a lattice constant of a = 45.0 Å ($a = 2d_{100}/\sqrt{3}$). Materials MCM-bpy and MCM-bpy-Mo, obtained after subsequent stepwise functionalization with bpy and the Mo complex, still show three reflections although with a slight deviation of the position maxima towards higher 2θ values as compared to MCM. For MCM-bpy material the d_{100} value is 35.5 Å with a corresponding lattice constant of a = 41.0 Å; for MCM-bpy-Mo the values are respectively d_{100} = 36.1 Å and a = 41.6 Å. The observed peak's intensity reduction is common to all materials; being higher in MCM-bpy-Mo. This is not due to a crystallinity loss, but rather due to an X-ray scattering contrast reduction between the silica walls and pore-filling material. This has been observed for other types of materials and is well described in the literature.[24,25]

All data is collected in Table 1, summarizing the relevant textural properties of all materials leading to their preparation.

Nitrogen sorption/desorption studies at 77 K were performed and have revealed that MCM samples exhibits a reversible type IV isotherm (Fig. 2a), typical of mesoporous solids (pore width between 2 nm and 50 nm, according to IUPAC).[26]

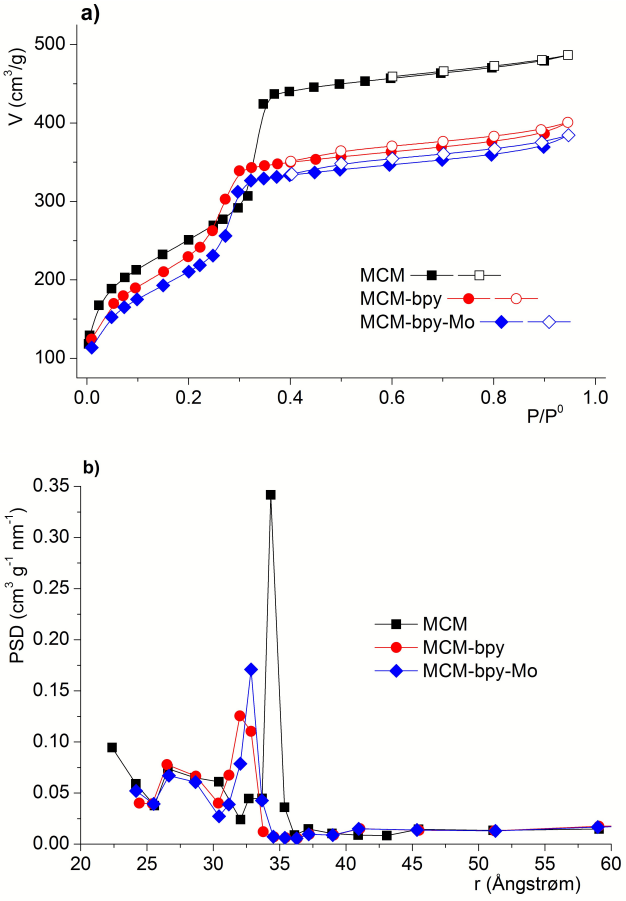

Figure 2. N_2 isotherms at 77K (a) and pore size distribution curves (b) for MCM, MCM-bpy and MCM-bpy-Mo materials. The N_2 isotherms display the sorption (closed symbols) and desorption (open symbols) branches.

The calculated textural parameters (S_{BET} and V_P) of these materials (Table 1) agree with literature data.[27,28] The capillary condensation/evaporation step in the pristine MCM sample appears in the 0.34–0.44 relative pressures range while the sharpness of this step reflects a uniform pore size distribution (Figure 2b).

Table 1. Textural parameters of host and composite materials, derived from powder XRD data and N_2 isotherms at 77 K, for all prepared mesoporous materials.

Material	2θ (º)	d_{100} (Å)	a (Å)	S_{BET} ($m^2\ g^{-1}$)	ΔS_{BET}[a] (%)	V_P ($cm^3\ g^{-1}$)	ΔV_P[b] (%)	d_{BJH} (Å)
MCM	2.26	39.0	45.0	897	–	0.75	–	34.3
MCM-bpy	2.47	35.5	41.0	819	-9	0.62	-17	32.8
MCM-bpy-Mo	2.49	36.1	41.6	755	-16	0.60	-21	31.9

[a] Surface area variation relatively to parent MCM material; [b] Total pore volume variation relatively to parent MCM material.

The functionalized material MCM-bpy isotherm revealed much lower N_2 uptake, accounting for the decreases in both S_{BET} (9%) and V_P (17%), according to Table 1. These findings indicated that the ligand immobilization on the internal silica surface was accomplished (Figure 2, Table 1). For the MCM-bpy-Mo material, the S_{BET} and V_P decrease in relation to MCM was 16% and 21%, respectively. These results were in agreement with the P/P^0 coordinate decrease on the isotherm inflection points after post-synthesis treatments.[29] Furthermore, the maxima of the PSD curves (Figure 2b) determined by the BJH method, d_{BJH}, for this series of materials changed from 34.3 Å to 31.9 Å (Table 1). The XRD powder patterns and textural parameters described above (Figure 2 and Table 1) were found to match the values reported in the literature for related systems.[12,30,31]

Catalytic studies

The catalytic activity of MCM-bpy-Mo in styrene epoxidation was tested using *t*-butylhydroperoxide (tbhp) as oxygen source at 353 K with addition of acetonitrile as solvent. The reaction kinetics was followed for 24 h and collected data are shown in Figure 3.

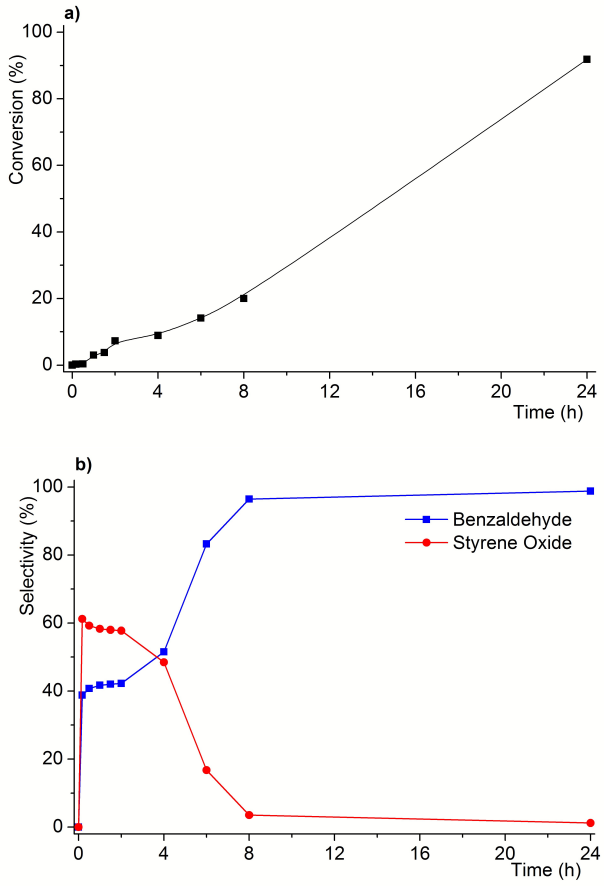

Figure 3. Styrene conversion (a) and styrene oxide and benzaldehyde selectivity (b) time-profiles for oxidation of styrene catalyzed by MCM-bpy-Mo.

The catalyst was found to be very efficient for styrene conversion, reaching 91% after 24 h (Figure 3a). Selectivity for the epoxide touched 60% in the first 2 h of reaction. After that time, the yield of the epoxide decreased dramatically while that of benzaldehyde rose concomitantly. This observation was compatible with the mechanism proposed in Scheme 1, where benzaldehyde was formed through an oxidative cleavage mechanism from over-oxidation of styrene epoxide. In addition, the kinetic data also show that (i) benzaldehyde was not produced directly by the Mo catalyst (its selectivity was lower in the initial reaction period) and (ii) there must be a critical level of epoxide to trigger the transformation. This catalytic test served as a benchmark for the DRIFT and INS studies discussed in the following sections.

DRIFT spectroscopy

Diffuse reflectance infrared spectroscopy (DRIFT) was used to characterize the catalyst and to provide insight into the working environment of the reaction. The DRIFT spectrum of the

fresh MCM-bpy-Mo catalyst, shown in Figure 4, is typical of a silicate evidencing a broad band in the 3600–2600 cm^{-1} range due to hydrogen bonding silanol groups.

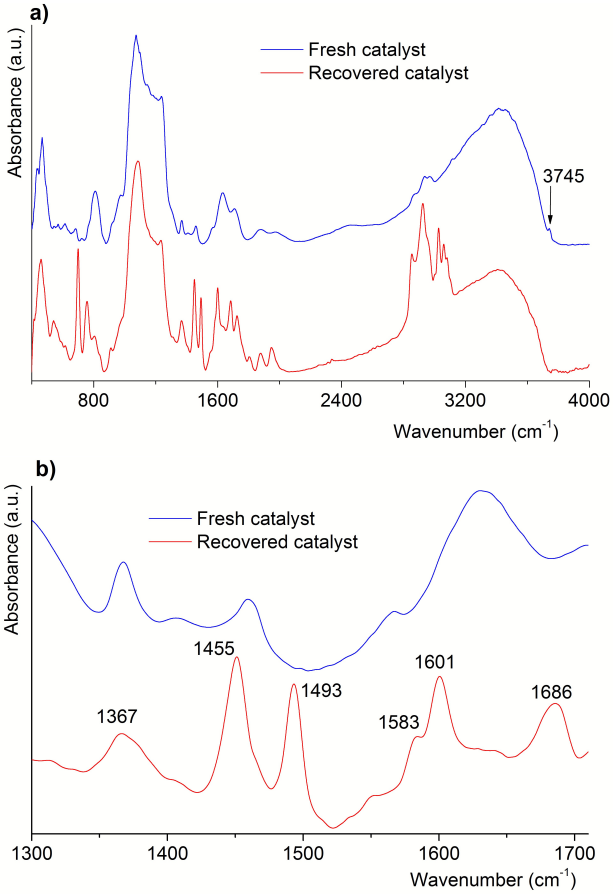

Figure 4. DRIFT spectra of fresh and recovered catalyst (at 4 h reaction time) in the complete mid-IR (a) and specific fingerprint (b) regions. The inset in (a) evidences the sharp band at 3745 cm^{-1} in the fresh catalyst.

In the fresh catalyst a sharp band at 3745 cm^{-1} is due to "free" silanol groups not involved in hydrogen bonding. Other important features comprise the intense broad band at 1239–950 cm^{-1} assigned to the asymmetric stretching vibration modes of the mesoporous framework (νSi–O–Si).[16] On the other hand, after running the catalytic reaction the recovered catalyst displayed a somewhat different profile with more spectral features. One of the major differences was the vanishing of the band assigned to "free" silanols. This was a good indication that there were adsorbed species at the surface of the host MCM material thus corroborating the mechanistic proposal (Scheme 1). In addition, in the νC–H mode region, there was a more complex pattern arising from the adsorbed species. The set of three bands at

3084, 3060 and 3026 cm^{-1} can be due to any of the compounds in the process – styrene, its epoxide and benzaldehyde. However, a sharp band at 2854 cm^{-1} denunciates clearly the presence of benzaldehyde inside the pores. In addition a feature at 2925 cm^{-1} is due to *t*-butanol, which is a by-product from the decomposition of tbhp.

To better assess the species adsorbed inside the pores of the catalyst, the fingerprint region was studied. Table 2 shows the bands found for the reference materials and those from the recovered catalyst after being active for 4 h.

Table 2. Assignment of vibrational modes for relevant species in the 1700–1300 cm^{-1} region at 298 K.

Styrene (neat)	Styrene oxide (neat)	Benzaldehyde (neat)	MCM-bpy-Mo (flowed, recovered)	Assignment
		1703	1686	νC=O
1630				νC=C
1601	1608	1597	1601	νC=C + δC−H
1576	1584	1584	1583	νC=C + δC−H
1495	1497		1493	δC−H + νC=C
	1477			
1449	1463	1456	1455	δC−H + νC=C
1412				δC−H (CH_2)
1334	1331	1339		δC−H + νC=C

Analysis of Table 2 and Figure 4b shows that in the recovered catalyst it is possible to identify bands associated with νC=C (1601 and 1583 cm^{-1}) and δC−H (1493 and 1452 cm^{-1}) typical from aromatic moieties. Comparison with the neat standards shows that the bands in the catalyst do not deviated significantly from the expected values. The band from the νC=C mode of styrene (1630 cm^{-1}) was absent in the spectrum of the recovered catalyst (Fig 4b). This indicates that there is not too much styrene adsorbed at the catalyst's surface. This could be anticipated since styrene does not have any oxygen atom and therefore specific interactions should be weaker. Another reason may be related to the fact that styrene is the reagent and was almost completely converted into products.

The major change is observed however for the νC=O mode arising from the presence of benzaldehyde. The neat compound displays this mode at 1703 cm^{-1}, while in the spectrum of

the recovered catalyst a band with a maximum at 1687 $cm^{-1}$was observed. The position of the band denoted a red-shift which was compatible with a strong interaction by hydrogen bonding where weakening of the C=O bond is expected. This interaction is anticipated to be established with single or germinal/vicinal silanols, which would give rise to distinct C=O bond lengths and concomitantly to different stretching vibrations towards lower frequencies. A similar situation is detected for styrene oxide. The epoxide ring breathing mode was expected at 877 cm^{-1}; however in the spectrum of the recovered catalyst no band was observed at those values. Instead a band at 909 cm^{-1} was detected which could be due to the interacting oxyrane ring through hydrogen bond. In this case a blue-shift was observed and that was due to the fact that since the ring is more hindered its frequency of vibration will rise. Still both C=O and oxyrane stretching modes in benzaldehyde and styrene oxide, respectively, experienced shift of the same magnitude, ca. 25 cm^{-1}. Looking at Figure 4b there is a band centered at 1367 cm^{-1} that is due to δO–H groups from the catalyst's surface. Compared to the fresh catalyst spectrum, this band displays a broader profile, most probably due to interactions with adsorbed species at the surface. This behaviour is compatible with the observations mentioned above for the carbonyl (benzaldehyde) and oxyrane (styrene epoxide) moieties.

For comparison purposes we have also collected the DRIFT spectra for the recovered catalyst after 2 h and 24 h of reaction time. The purpose was to have a clearer picture of whether the spectra would be closer to styrene oxide and benzaldehyde, respectively, since at the mentioned reaction times those products would be major. In fact, clear differences between both recorded spectra after 2 and 24 h were observed (Figure S1), stressing the point that DRIFT can probe each of the products. In addition, each of these spectra was found to be different from that shown in Fig. 4b, which was recorded after 4 h reaction time, when product selectivity is roughly 50% for each product.

Inelastic neutron scattering spectroscopy

INS was measured on TOSCA for both the fresh and the recovered catalyst. Figure 5, shows the spectra of the mentioned samples across the energy range between 20–4000 cm^{-1}, while Figure 6 shows the corresponding spectra in the fingerprint region. Reference spectra of pure styrene, styrene oxide and benzaldehyde in the same regions are shown in the ESI (Figures S2 and S3).

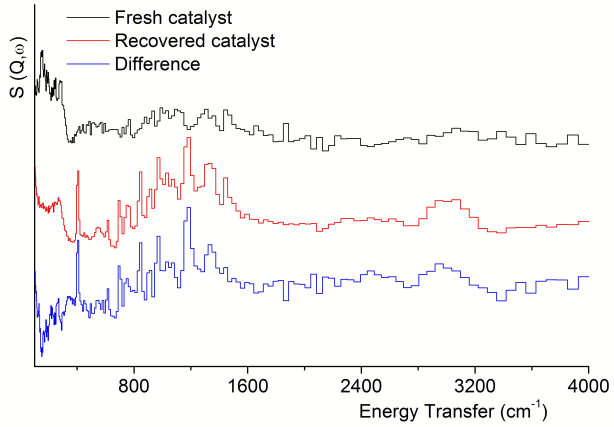

Figure 5. INS spectra of the fresh catalyst (a), recovered catalyst after styrene oxidation catalysis at 353 K for 4 h (b) and difference spectra. Spectra (a) and (b) were normalized prior to calculation of the difference.

In Figures 5 and 6 striking differences can be observed. The INS spectrum of fresh MCM-bpy-Mo catalyst shows weak spectral features, which were consistent with the low loading of guest species. On the other hand the recovered catalyst shows several new bands with much higher intensity.

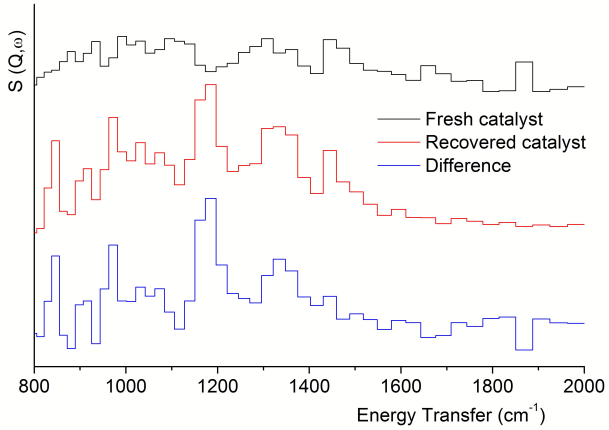

Figure 6. INS spectra in the fingerprint region of the fresh catalyst (a), recovered catalyst after styrene oxidation catalysis at 353 K for 4 h (b) and difference spectra. Spectra (a) and (b) were normalized prior to calculation of the difference.

The difference spectrum shows the persistence of several features in the fingerprint region. Comparison with the reference spectra, Figs. S2 and S3 (ESI†), showed clearly that there was a mixture of both species contributing to the INS spectrum. This suggested, as expected, that

for this particular MCM-41 based system INS was probing all the species inside the channels of the catalyst that were active players in the catalytic process. Caution should prevail here, since the previous statement should be true for catalysts with high surface area and with easily accessible porous systems such as those based on MCM-41 supports. This is because INS (and DRIFT) are not surface sensitive techniques.

Assuming styrene oxide and benzaldehyde to be present in high concentration (50% selectivity after 4 h reaction time, according to the measured reaction kinetics, Figure 3) there were differences in the adsorbed species compared to the spectrum of the neat compound. As evidenced in Figure 7, the band at 1200 cm^{-1}, assigned to CH deformation modes, was blue-shifted from its original position. This behaviour was consistent with hydrogen bonding of such groups, through C—H···O interactions,[33] with the surface of the catalyst.

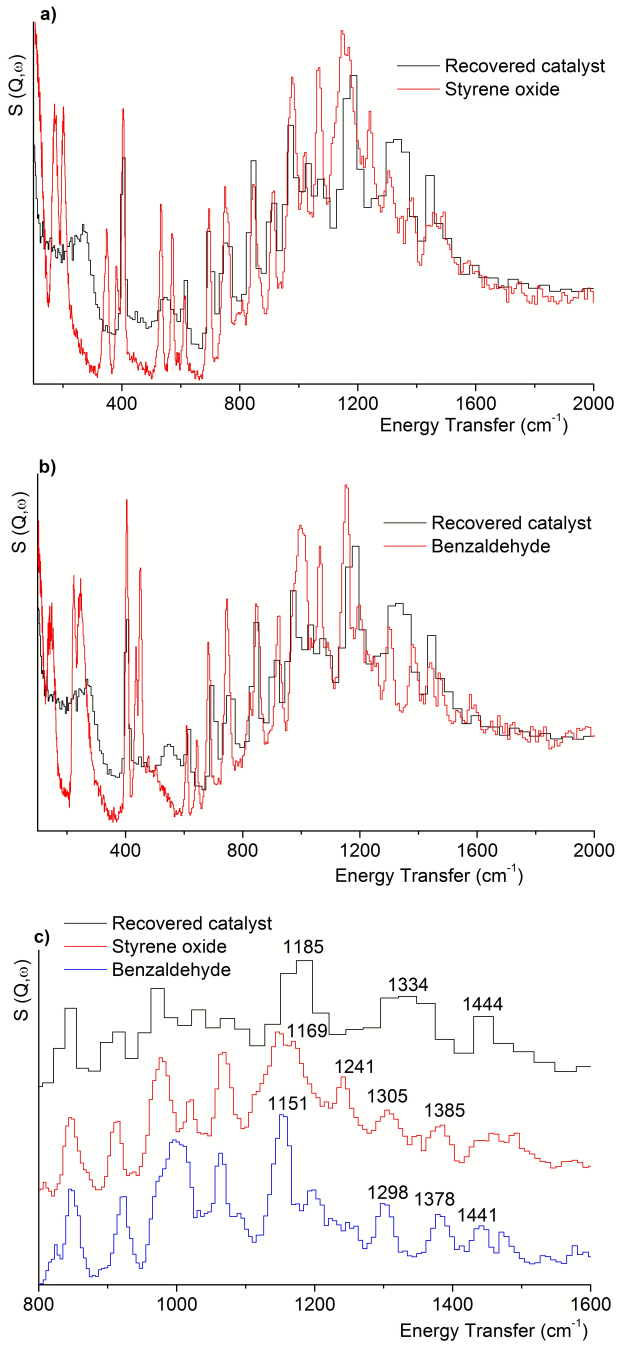

Figure 7. Comparison of the INS spectra of recovered catalyst and styrene oxide (a) and benzaldehyde (b) in the region 100–2000 cm^{-1}. Comparison of INS spectra of neat compounds with that of the recovered catalyst is shown in c) for the fingerprint region; special attention should be paid to the bands above 1100 cm^{-1} which show more dramatic changes (see discussion in the text).

By the same token, another strong feature at ~1400 cm^{-1} was also blue-shifted from its position in styrene oxide. However, this band could also be assigned to benzaldehyde, which also revealed a strong feature in this region at lower wavenumbers.

At this point the complementarity of DRIFT and INS should be stressed out. In fact while INS could effectively probe easily deformation CH modes involved in host-guest interactions by means of hydrogen bonding, DRIFT provided information about the modes that are not observed in INS. These include the νC=O and the oxirane ring modes from benzaldehyde and styrene oxide, respectively. In this way, under hydrogen bonding regime the CH deformation modes would experience a blue-shift (which is observed with INS) whereas the for benzaldehyde one would expect a red-shift of the carbonyl mode. This was confirmed by DRIFT as well as the blue-shift of the oxirane breathing mode, as discussed above.

The presence of styrene was not easily probed, being understandable, since styrene was being converted into its oxidation products (Figure 4) and also because after 4 h reaction the system was flushed to remove weakly bound pecies. From these data one can assume that at a given point in time during the oxidation reaction of styrene, there was a mixture of oxidation products adsorbed at the surface of the MCM channels and this could be probed by INS, based on the time of reaction (4 h, see Figure 4b). Actually this could be expected as oxidation products (styrene oxide and benzaldehyde) hold "O" atoms; in addition such findings corroborate the DRIFT data discussed above. This leads to stronger host-guest interactions that make possible the measurement of such surface species by INS. On the other hand, because styrene does not have any electronegative nuclei (e.g. N or O) it is a species that should not have strong interactions with the surface of the catalyst. Therefore, after the system being flushed, little adsorption was expected and that was why it was probed with more difficulty in this study.

Although caution should always prevail, we have tested an interesting exercise where we tried to estimate the relative amounts of the reaction products inside the pores of the used catalyst. This relied on a Job-plot method where the ends are the measured spectra from neat styrene oxide and benzaldehyde, while the middle points are assessed by blending both spectra from those species. The next step was achieved, after spectra normalization to unit area) by subtracting these neat/blended spectra from the INS spectrum of the used catalyst in the spectral region between 100−2000 cm^{-1}. The result is shown in Figure 8a. Afterwards, the area of each difference spectrum was calculated and plotted against the molar fraction of styrene oxide. Where the Job-plot was minimized it would indicate the best match of the blended styrene oxide/benzaldehyde spectra.

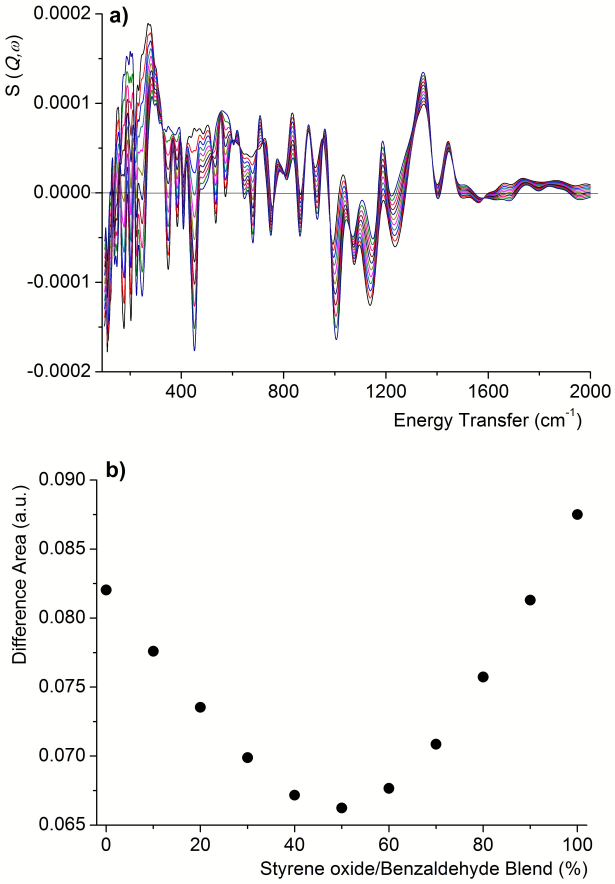

Figure 8. (a) INS difference spectra between the spectrum of the recovered catalyst after 4 h reaction time and the neat/blended spectra of styrene oxide and benzaldehyde; (b) Job-plot shows the calculated area of each difference spectrum against the corresponding quantity of styrene oxide in the blend. The minimum value corresponds to the best match.

The result, shown in Figure 8b, evidences a Job-plot whose minimum was found between 40-60% (accounting for obvious errors in the approach). This result was in excellent agreement with the time-resolved selectivity of styrene oxide/benzaldehyde throughout the catalytic reaction. As can be seen in Figure 3b, the selectivity vs. time profile shows that after 4 h the experimentally measured selectivity was 45%. Such result shows a very good agreement with the Job-plot result, although caution should always prevail in this conclusion as several assumptions were made.

Nevertheless, this study evidences the powerfulness of INS in probing guest species inside porous supports that act as catalysts compared to other common techniques such as FTIR or Raman.

Concluding remarks

In this work we have assessed the surface species after styrene oxidation on a composite epoxidation catalyst based on MCM-41 with immobilized Mo complexes. Previous experiments demonstrated that styrene oxidation with this catalyst yields styrene oxide, which then undergoes oxidative cleavage leading to high yields of benzaldehyde. The maximum selectivity for styrene oxide had been estimated at ca. 4 h reaction time and after that there is the inter-conversion into benzaldehyde that is obtained almost exclusively after 24 h. INS allowed for some insight into what lies inside the pores of the catalyst as follows: The overall spectrum of the recovered catalyst shows an intricate set of bands whose origin can be assigned to the presence of styrene, styrene oxide and benzaldehyde. Concerning benzaldehyde and styrene oxide, these seem to have a higher contribution to the overall spectrum as compared to styrene; this is most probably due to the fact that those compounds hold strong acceptor groups that can establish hydrogen bonds, whereas styrene does not. INS allowed for estimation of product selectivity in the catalyst by means of a Job method. Despite being a somewhat novel approach in INS, this has been previously applied sucessfuly to address hydrogen bond stoichiometry.[33] Although the present approach must be taken with care, there is a very good match with experimental kinetic data.

Agreement between INS and DRIFT measurements is excellent with complimentary data being gathered by each technique. In particular while INS allowed to probe which specific modes involving CH or CH_2 donor groups were bound to the surface, by hydrogen bonding, DRIFT spectroscopy, on the other hand probed quite nicely the effects of hydrogen bonding on both carbonyl and oxirane acceptor groups in benzaldehyde and styrene oxide, respectively. In this way this work showed how DRIFT and INS can effectively complement each other and provide a clear picture of catalysts *in operando* conditions. We should once more alert to the fact that any of the technique is not surface specific, meaning that they will not distinguish species that are either on the inside or outside of a given catalyst.

Further work is currently ongoing to explore the capabilities of neutron scattering techniques in probing surface species in similar systems designed for oxidation processes.

Acknowledgements

Authors thank FCT, POCI and FEDER (project UID/MULTI/00612/2013) for financial support. CIF also thanks FCT for a research grant (SFRH/BD/81029/2011) and RSC for a visiting scientist fellowship at ISIS. The authors thank the STFC Rutherford Appleton Laboratory for access to ISIS Pulsed Neutron and Muon Source facility. Authors also thank support by the European Commission under the 7th Framework Programme through the

'Research Infrastructures' action of the 'Capacities' Programme, NMI3-II Grant number 283883. Contract No. 283883-NMI3-II.

References

[1] G.A. Somorjai, *Top. Catal.*, 2008, **48**, 1–7.

[2] A. Corma and H. Garcia, *Top. Catal.*, 2008, **48**, 8–31.

[3] A. Taguchi and F. Schüth, *Micropor. Mesopor. Mater.*, 2005, **77**, 1-45.

[4] M.H. Valkenberg and W.F. Hölderich, *Catal. Rev. – Sci. Eng.*, 2002, **44**, 321-374.

[5] F. Hoffmann, M. Cornelius, J. Morell and M. Fröba, *Angew. Chem. Int. Ed. Engl.*, 2006 **45**, 3216-3251.

[6] C. I. Fernandes, G. B. G. Stenning, J. D. Taylor, C. D. Nunes and P. D. Vaz, *Adv. Synth. Catal.*, 2015, **357**, 3127-3140.

[7] R. A. Sheldon and J. K. Kochi, *Metal-Catalysed Oxidations of Organic Compounds*, Academic Press, New York, 1981.

[8] M. Hudlicky, *Oxidation in Organic Chemistry*, American Chemical Society, Washington, DC, 1990.

[9] T. Mallat and A. Baiker, *Chem. Rev.*, 2004, **104**, 3037–3058.

[10] E. Nowicka, J. P. Hofmann, S. F. Parker, M. Sankar, G. M. Lari, S. A. Kondrat, D. W. Knight, D. Bethell, B. M. Weckhuysen and G. J. Hutchings, *Phys.Chem. Chem. Phys.*, 2013, **15**, 12147-12155.

[11] C. I. Fernandes, N. U. Silva, P. D. Vaz, T. G. Nunes and C. D. Nunes, *Appl. Catal. A: Gen.*, 2010, **384**, 84-93.

[12] N. U. Silva, C. I. Fernandes, T. G. Nunes, M. S. Saraiva, C. D. Nunes and P. D. Vaz, *Appl. Catal. A: Gen.*, 2011, **408**, 105-116.

[13] B. Feng, Z. Hou, X. Wang, Y. Hu, H. Li and Yunxiang Qiao, *Green Chem.*, 2009, **11**, 1446–1452

[14] M.R. Mayura, U. Kumar and P. Manikandan, *Dalton Trans.*, **2006**, 3561–3575.

[15] M.R. Mayura, M. Kumar and S. Sikarwar, *React. Funct. Polym.*, 2006, **66**, 808–818.

[16] P. D. Vaz, C. D. Nunes, M. Vasconcellos-Dias, M. M. Nolasco, P. J. A. Ribeiro Claro and M. J. Calhorda, *Chem. Eur. J.*, 2007, **13**, 7874-7882.

[17] P.K. Baker, *Chem. Soc. Rev.*, 1998, **27**, 125–132.

[18] N. Garelli and P. Vierling, *J. Org. Chem.*, 1992, **57**, 3046-3051.

[19] C.D. Nunes, A.A. Valente, M. Pillinger, A.C. Fernandes, C.C. Romão, J. Rocha and I.S. Gonçalves, *J. Mater. Chem.*, 2002, **12**, 1735-1742.

[20] M. Kruk, M. Jaroniec and A. Sayari, *Langmuir*, 1997, **13**, 6267-6273.

[21] M. Kruk, V. Antochshuk, M. Jaroniec and, A. Sayari, *J. Phys. Chem. B*, 1999, **103**, 10670-10678.

[22] D Colognesi, M Celli, F Cilloco, R J Newport, S F Parker, V Rossi-Albertini, F Sacchetti, J Tomkinson and M Zoppi, *Appl. Phys. A*, 2002, **74**, S64-S66.

[23] SF Parker, F Fernandez-Alonso, AJ Ramirez-Cuesta, J Tomkinson, S Rudic, RS Pinna, G Gorini and J Fernández Castañon, *J. Phys.: Conf. Ser.*, 2014, **554**, 012003.

[24] B. Marler, U. Oberhagemann, S. Voltmann and H. Gies, *Micropor. Mater.*, 1996, **6**, 375.

[25] W. Hammond, E. Prouzet, S.D. Mahanti and T.J. Pinnavaia, *Micropor. Mesopor. Mater.*, 1999, **27**, 19-25.

[26] S.J. Gregg and K.S.W. Sing, *Adsorption, Surface Area and Porosity*, Academic Press, London, 1982.

[27] M.D. Alba, A. Becerro and J. Klinowski, *J. Chem. Soc., Faraday Trans.*, 1996, **92**, 849-854.

[28] A.A. Romero, M.D. Alba, W. Zhou and J. Klinowski, *J. Phys. Chem. B*, 1997, **101**, 5294–5300.

[29] M. Kruk and M. Jaroniec, *Langmuir* 1999, **15**, 5410-5413.

[30] N.U. Silva, T.G. Nunes, M.S. Saraiva, M.S. Shalamzari, P.D. Vaz, O.C. Monteiro and C.D. Nunes, *Appl. Catal. B*, 2012, **113–114**, 180-191.

[32] A.C. Ventura, C.I. Fernandes, M.S. Saraiva, T.G. Nunes, P.D. Vaz and C.D. Nunes, *Curr. Inorg. Chem.*, 2011, **1**, 156-165.

[33] P. D. Vaz, M. M. Nolasco, F. P. S. C. Gil, P. J. A. Ribeiro-Claro and J. Tomkinson, *Chem. Eur. J.*, 2010, **16**, 9010 – 9017.